

Optical properties of laser-melt-quenched Au-Si alloys

E. Huber and M. von Allmen

Institute of Applied Physics, University of Bern, CH-3012 Bern, Switzerland

(Received 4 February 1983; revised manuscript received 2 June 1983)

Glassy films of Au-Si alloys were produced by nanosecond laser quenching in the composition range from 25–93 at. % Si. Reflection and transmission coefficients as well as electrical conductivity were measured from 1.4 to 5.4 eV. The complex dielectric function, obtained from Kramers-Kronig analysis, is presented. The optical properties of the Au-Si system over the whole phase diagram can be described using a Lorentz-Drude model with a free-electron term and a single-resonance bound-electron term. We conclude that two electronic transitions occur in the system: Si switches between the metallic and the semiconducting state at about 30 at. % Si, whereas Au switches from the metallic to a dielectric state at about 85 at. % Si. These two transitions of the constituents separate three regions of markedly different electronic behavior in the alloy.

I. INTRODUCTION

Glassy alloys offer the possibility to study the ways in which unmiscible atomic species influence each other when in close contact. The system Au-Si at its eutectic composition (19 at. % Si) is a well-known glass former by splat cooling. However, the glass forming ability of a mixture is known to decrease if the composition is changed away from the eutectic. This limits the compositional range of glasses available by mechanical melt quenching to a range close to the eutectic.

Laser quenching with its much higher cooling rate¹ enables glass formation from the liquid state over most of the Au-Si phase diagram. Glassy phases in the composition range between 9 and 91 at. % Si have first been demonstrated by von Allmen *et al.*² This for the first time enables a study of melt-quenched Au-Si over the entire range of compositions. This is the objective of the present investigation.

Vapor quenching has previously been used to produce Au-Si amorphous phases over most of the phase diagram.^{3–7} These investigations have shown that in metal-rich amorphous alloys of Si with Au (as well as with other noble metals) the Si atom is in a metallic state, as demonstrated by Hiraki *et al.*⁸ The same behavior was found for Ge by Stritzker and Wühl.⁹ Mangin *et al.*³ pointed out that the Au-rich alloys have a close-packed metallic structure. The optical and electrical properties of Au-rich alloys have been investigated by Hauser *et al.*⁴ and Hauser and Tauc.⁵ The metal-semiconductor transition in the Si-rich alloys was investigated by Hauser *et al.*⁶ and also by Nishida *et al.*⁷ and by Morigaki.¹⁰

For the Si-rich alloys (Si concentration ≥ 50 at. %) there are, as will be shown below, marked differences between our optical results and those of Ref. 4. We believe that these differences reflect different structural properties of the vapor-quenched and melt-quenched phases. It may be pointed out that vapor-quenched Si-rich “glasses” show higher crystallization temperatures³ (140°C at 50 at. % Si and 200°C at 85 at. % Si) than liquid-quenched ones (below 100°C from 25 to 85 at. % Si).² On the other hand, Hauser *et al.* showed⁶ that for compositions between 15

and 40 at. % Si the electrical conductivities are quite similar in the liquid and in the (vapor-quenched) amorphous state.

II. EXPERIMENTAL PROCEDURE AND RESULTS

Samples were prepared by electron-gun deposition of alternating layers of Au and Si onto sapphire substrates in a vacuum better than 10^{-7} mbar. The thicknesses of the individual layers were chosen such as to yield the desired mean composition after laser melting and interdiffusion. In order to ensure homogeneous mixing, individual layers were made no more than 30 nm thick. Overall thickness was about 200 nm. These structures were irradiated with 30-ns pulses from a Nd:YAG (yttrium aluminum garnet) laser. With these parameters relevant cooling rates are of the order of 10^{10} K/s.¹

The amorphousness was established by both x-ray diffraction and conductivity measurements. Glasses of Si-rich composition are stable at room temperature, whereas Au-rich ones tend to recrystallize and must be kept at re-

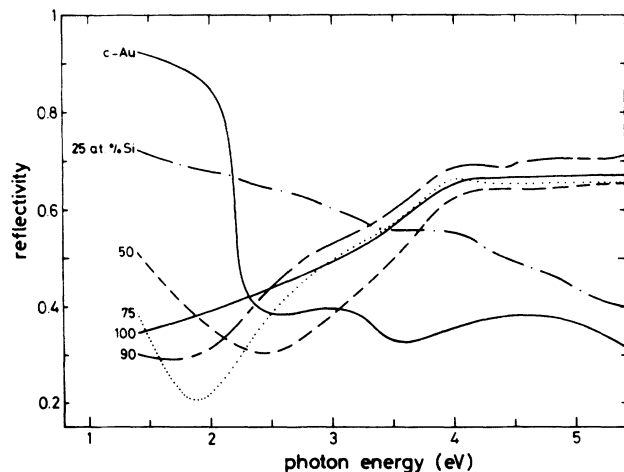


FIG. 1. Measured reflectivities of laser-quenched glassy Au-Si films. The pure elements were vapor deposited; Au is crystalline while Si is amorphous.

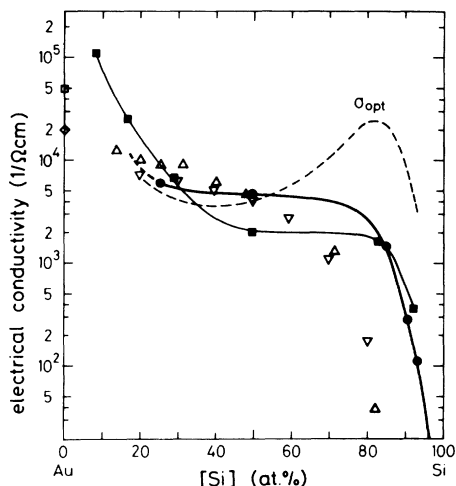


FIG. 2. Measured electrical conductivity of glassy Au-Si films. The following symbols are used: ●, laser quenched (this work); ■, laser quenched by von Allmen (Ref. 13); ▽ (Ref. 3) and △ (Ref. 6), vapor quenched; ◇, vapor quenched Au, deposition temperature 25 K (Ref. 14), □, liquid Au extrapolated to room temperature (Ref. 16). The dashed line was calculated from the optical properties using Eq. (8).

duced temperature. Some samples were annealed to induce crystallization before measurement. Measurements of reflection and transmission coefficients were performed with a spectrophotometer Cary 219 at photon energies ranging from 1.4 to 5.4 eV. The Si-rich films have low absorption, and measured reflection values were corrected for interference effects using the exact formulas.¹¹ Electrical conductivity was measured with a four-point probe.

Figure 1 shows reflectivity spectra for various glass compositions; also included are spectra for pure Si (amorphous, vapor deposited) and for pure Au (crystalline). A spectrum of liquid Au, extrapolated to room temperature might be more appropriate, but since the optical properties of solid and liquid Au do not differ significantly, as reported by Miller,¹² and in order to avoid extrapolation over more than 1000 K, we always consider crystalline Au.

Figure 2 shows the dc conductivity σ_0 as a function of composition for the same films; also included are the first measurements of laser-quenched Au-Si glasses by von Allmen and Mäenpää¹³ as well as measurements of vapor-quenched amorphous phases by Mangin *et al.*³ and Hauser *et al.*⁶ The conductivity of amorphous Au was given by Hauser *et al.*¹⁴ They used getter sputtering in He gas at a temperature of 25 K. Similar measurements were performed by Swenumson and Even.¹⁵ For comparison a value for liquid Au, extrapolated to room temperature¹⁶ is also given. Three regions with strongly different slopes of conductivity versus composition can be distinguished in Fig. 2; in the medium composition range the conductivity is roughly constant at about $5 \times 10^3 (\Omega \text{ cm})^{-1}$. The dashed line was calculated from the optical properties as described below.

III. MODELING OF THE DIELECTRIC FUNCTION

In this section we analyze the data of Fig. 1 on the basis of various models of the Au-Si system. Perhaps the sim-

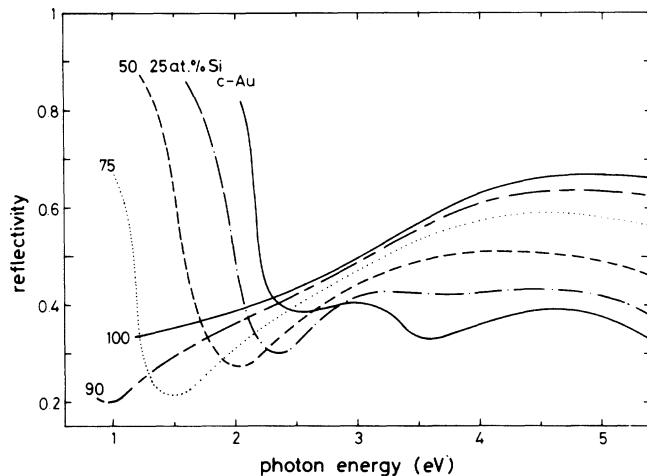


FIG. 3. Reflectivity calculated from a linear combination of the dielectric functions of pure (crystalline) Au and pure (amorphous) Si.

plest possible model consists in neglecting any interaction between the Au and Si atoms. We thus write the dielectric function for a film of given concentration x as a linear combination of the dielectric functions of the elements

$$\epsilon(\omega) = x\epsilon_{\text{Si}}(\omega) + (1-x)\epsilon_{\text{Au}}(\omega), \quad (1)$$

where x is expressed in atomic fraction of Si. The dielectric function of pure amorphous Si to be used in (1) was measured separately. The dielectric function of crystalline Au was calculated from reflectivity data reported by Ackermann *et al.*¹⁷ The reflectivity can be calculated from

$$R = \frac{1 - [2(\epsilon_1 + |\epsilon|)]^{1/2} + |\epsilon|}{1 + [2(\epsilon_1 + |\epsilon|)]^{1/2} + |\epsilon|}, \quad (2)$$

where $|\epsilon| = (\epsilon_1^2 + \epsilon_2^2)^{1/2}$, $\epsilon_1 = \text{Re}\epsilon$, and $\epsilon_2 = \text{Im}\epsilon$.

Figure 3 shows a few such calculated spectra. By comparing with Fig. 1 we note that one important feature of the measured spectra, the occurrence of a reflectivity minimum and its shifting to lower energies with increasing Si content, is correctly described by this simple model, although the actual relaxation times are smaller than those predicted. However, particularly for compositions of less than 50 and more than 80 at. % Si, agreement with the linear model [Eq. (1)] is quite poor. For annealed samples with a phase-separated crystalline equilibrium structure the agreement, as expected, is much better.

In order to get a better description we use a classical (Lorentz-Drude-type) expression for the dielectric function, with electron densities and damping constants that are fitted to the measured reflectivity curves. We allow for electrons in three different states: free electrons, electrons in the d band of Au, and electrons in virtual bound states (VBS) contributed by Si. According to this we write for a given composition

$$\epsilon(\omega) = \epsilon^b(\omega) + \epsilon^f(\omega) + \delta\epsilon(\omega). \quad (3)$$

Here ϵ^b is the contribution of the electrons in the VBS and ϵ^f the free-electron contribution. $\delta\epsilon$ describes the influence of the Au d band. These three terms in (3) are described as follows.

In the *VBS model* the optical properties of the Si atoms are described by equivalent Lorentz oscillators.¹⁸ In contrast to the behavior of pure crystalline Si where two significant resonance peaks at 3.4 and 4.3 eV are observed¹⁹ there is only one strongly damped resonance (at 3.4 eV) in amorphous Si, as demonstrated by Pierce and Spicer²⁰ and confirmed by our own measurements [see Fig. 6(b) below]. In our Au-Si glasses we will thus describe the Si atoms in terms of the VBS model with the resonant state at 3.4 eV, which corresponds to the direct bandgap of Si. The bound electron density and the damping constant are treated as parameters.

Free electrons are described by a Drude term with the electron density and the relaxation time as parameters.

The *d band* of Au modifies the free-electron reflectivity in two ways: First, it screens the plasma oscillation; provided the screened plasma frequency ω_p^* is lower than the onset of interband transitions from the *d* band, we have²¹

$$(\omega_p^*)^2 = \frac{4\pi n e^2}{m_0} \frac{1}{1 + \delta\epsilon(0)}, \quad (4)$$

where n is the free-electron density and m_0 the free-electron mass. $\delta\epsilon(0)$ denotes the *d*-band correction below the onset of interband transitions, where it is real. Second, at frequencies above the onset of transitions from the *d* band into the conduction band the free-electron density is increased by the extra electrons and hence the reflectivity is higher than expected from the free-electron density at low energies.

The *d*-band correction $\delta\epsilon(\omega)$ for pure crystalline Au was determined empirically from the reflectivity data given by Ackermann *et al.*¹⁷ and others.²² The procedure, as described by Ehrenreich and Philipp,²¹ requires the knowledge of the dielectric function in the infrared, far below the onset of *d* band transitions. Such measurements were not available for our Au-Si glasses, and the *d*-band correction was estimated using the fitting procedure discussed below. This showed that its inclusion was only appropriate for pure Au. Hence we will further omit the *d*-band correction for $x > 0$.

Equation (3) can now be written as

$$\epsilon(\omega) = 1 + \frac{4\pi e^2}{m_0} \left[\frac{n_b^*}{\omega_0^2 - \omega^2 - i\Gamma\omega} - \frac{n_f^*}{\omega(\omega + i/\tau)} \right], \quad (5)$$

where n_b^* is the effective density of electrons bound in the VBS, Γ the damping of this resonant state, n_f^* the effective density of free electrons, and τ the relaxation time of the free electrons. Effective densities are defined as

$$n^* = nm_0/m^*, \quad (6)$$

where m^* is the effective mass. Curve fitting is now used to extract values of n_b^* , n_f^* , Γ , and τ from the experimental curves of Fig. 1.

This model turns out to describe the system Au-Si very accurately over the whole phase diagram. The mean deviation between the fitted model and the measured reflectivity is about 2.5%. The agreement is somewhat better in the ranges from 0–50 at. % Si and from 90–100 at. % Si than in between. Figure 4 shows measured and theoretical reflectivities for 25 and 50 at. % Si as typical examples.

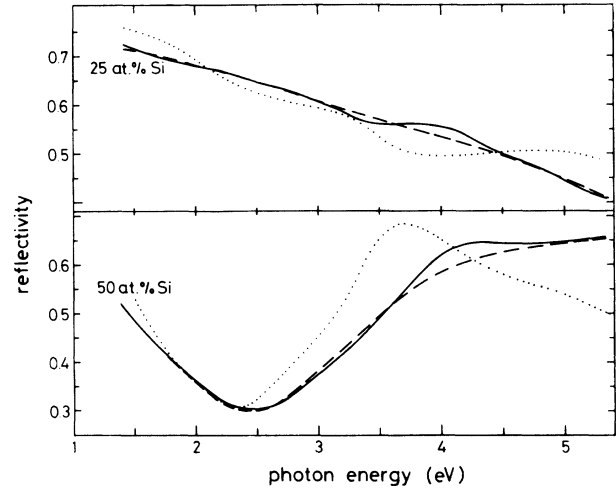


FIG. 4. Comparison between measured and fitted reflectivities of glassy Au-Si films. Full lines are measurements; dashed lines are fit with Eqs. (2) and (5); dotted lines are fit including *d*-band correction of pure Au weighted with Au concentration.

The full lines represent the measurements. The dashed lines are calculated from Eq. (5). The dotted lines show the best fit available if the *d*-band correction $\delta\epsilon$ for pure Au, weighted with the Au concentration, is added to (5). As this correction seems inappropriate, we drop the *d*-band correction, as mentioned above.

Figure 5 shows the effective densities n_b^* and n_f^* of bound and free electrons, respectively, as a function of concentration as obtained from the fitting procedure. The values adopted for the pure elements were chosen according to the following considerations.

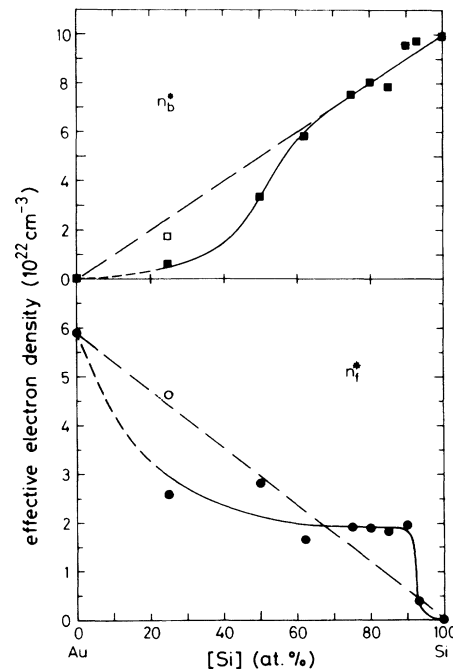


FIG. 5. Effective bound- and free-electron densities of glassy Au-Si films, extracted from fitting Eqs. (2) and (5) to the measured reflectivity. Open symbols denote a sample which was annealed to induce crystallization.

In the case of *pure Au* n_b^* is assumed to be zero. The free-electron density in the liquid state was determined to be exactly the atomic density, $5.9 \times 10^{22} \text{ cm}^{-3}$, as reported by Künzi and Güntherodt.²³ Since the liquid state is similar to the glassy state we adopt this value for n_f^* . Incidentally the value determined from the optical data of crystalline Au (Refs. 17 and 22) is very close, $5.7 \times 10^{22} \text{ cm}^{-3}$.

In the case of *pure Si* our optical measurements of vapor-deposited films lead to a value of n_b^* of about $1 \times 10^{23} \text{ cm}^{-3}$, i.e., two electrons per atom.²⁴ The effective density of free electrons n_f^* is assumed to be zero.²⁵ This was verified by fitting expression (5) to the pure Si reflectivity.

IV. KRAMERS-KRONIG ANALYSIS

As a further result of the above-mentioned fit, the dielectric functions of the glassy Au-Si films were determined by a Kramers-Kronig analysis, using Eq. (5) with the fitted parameters for a reliable extrapolation. The following equation was used to calculate the complex dielectric function:

$$\Theta(\omega) = -\frac{1}{2\pi} \int_0^\infty \ln \left| \frac{z+\omega}{z-\omega} \right| \frac{d}{dz} \ln R(z) dz, \quad (7)$$

where $\Theta(\omega)$ is the phase of the reflected wave, and $R(z)$ the reflectivity as a function of frequency. From 0 to 1.5 eV and from 5.4 eV to ∞ , $R(z)$ was extrapolated with the aid of Eqs. (2) and (5). Figures 6(a) and 6(b) show the complex dielectric function ϵ of Au-Si for several compositions (full lines); $\text{Re}\epsilon$ is shown in Fig. 6(a) and $\text{Im}\epsilon$ in Fig. 6(b). The dashed lines were directly calculated from Eq. (5) with the fitted parameters. The curves for pure crystalline Au were calculated from extended measurements by Ackermann *et al.*¹⁷ and others²² in order to avoid the need for extrapolation. The dielectric function was then compared with the results of Lässer and Smith²⁶ and Aspnes *et al.*²⁷ to test the integration procedure. No significant deviation was detected.

From the imaginary part of the dielectric function, as shown in Fig. 6(b), two main features of the system Au-Si can be seen. First, the *d* band of Au causes two peaks in the imaginary part of the dielectric function for pure Au, as shown in Fig. 6(b) (topmost). Interband transitions set in at about 2 eV. However, the influence of the *d* band disappears when 25 or 50 at. % Si is added. This may be due to the fact that the onset of interband transitions is shifted to higher energies, as Hauser *et al.* suggested.⁴ Second, resonance absorption by the virtual bound state of Si becomes dominant for concentrations higher than about 40 at. % Si. With further increasing Si concentration this resonance seems to split, as suggested by the shape of $\text{Im}\epsilon$ for 75 and 90 at. % in Fig. 6(b). We cannot presently offer a physical explanation for this behavior.

V. DISCUSSION

The fitted Lorentz-Drude model expressed in (5) has been shown to describe the optical properties of the system Au-Si very well. On physical grounds, the behavior of the effective electron densities shown in Fig. 5, as well as the

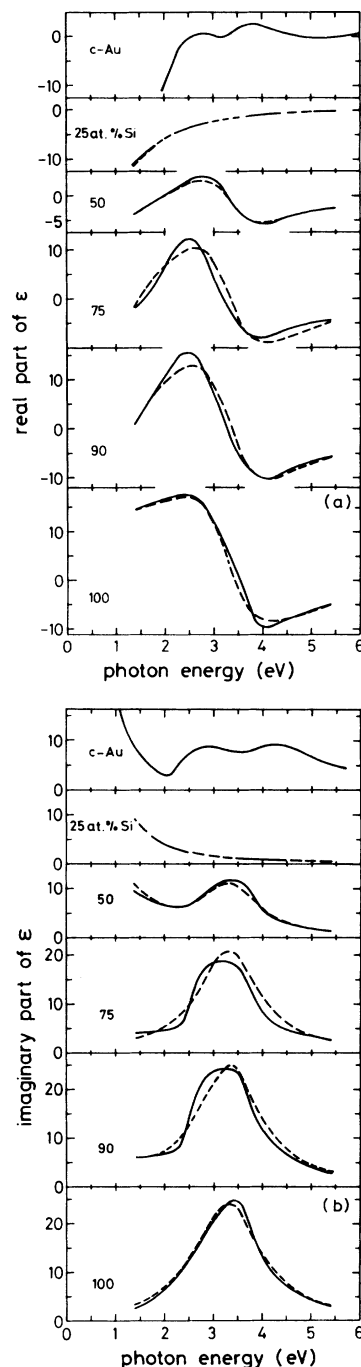


FIG. 6. Complex dielectric function of glassy Au-Si films, (a) real part and (b) imaginary part. The solid lines are calculated with Kramers-Kronig analysis and the dashed lines were calculated with Eq. (5) using the fitted parameters.

electrical conductivity σ_0 , as shown in Fig. 2, is dominated by two transitions in the electronic properties. Starting at the Au-rich end of the phase diagram, the first transition occurs at a composition of the order of $x_{ms} = 30$ at. % Si (where the n_b^* and σ_0 curves show a kink) and is due to the Si which behaves as a metal at lower and as a semiconductor at higher concentrations. Such a transition was also found in vapor-quenched Au-Si at 30 at. % Si by Hiraki *et al.*⁸ Further, Mangin *et al.*³ demonstrated that

the amorphous Au-Si alloys have a close-packed metallic structure up to 40 at. % Si while Hauser and Tauc⁵ showed that above 30–40 at. % the Si atoms become tetrahedrally coordinated. Au-Si glasses at the transition concentration x_{ms} have an electrical conductivity of $(5-6) \times 10^3 (\Omega \text{ cm})^{-1}$ in accordance with the value given by Mooij for the “saturation” conductivity of disordered metallic alloys.²⁸ The general shape of σ_0 versus composition on the Au-rich side resembles that found in other alloys between a good and a bad conductor, such as Au-Sn reported by Cote and Meisel.²⁹ Based on this similarity a rough estimate for the conductivity of the metallic state of Si may be obtained by comparing the related systems Au-Si and Au-Sn: In amorphous Au-Sn the concentration 35 at. % Sn (where Au-Sn shows a minimum of conductivity) may be considered equivalent to the transition concentration x_{ms} in the Au-Si system. At 35 at. % Sn the conductivity of Au-Sn is lower than that of pure liquid Sn (extrapolated to room temperature) by a factor of 2. Hence we would expect that the conductivity of the metallic state of Si is also about twice the value at the concentration x_{ms} , or about $1 \times 10^4 (\Omega \text{ cm})^{-1}$. For comparison, liquid Si which is well known to be metallic has a conductivity (at the melting point) of $1.2 \times 10^4 (\Omega \text{ cm})^{-1}$.³⁰ Further, the conductivity of the metallic state of Ge in amorphous Au-Ge alloys was estimated by Stritzker and Wühl to $1 \times 10^4 (\Omega \text{ cm})^{-1}$ (Ref. 9) and that of liquid Ge was reported by Dreirach *et al.* to $1.5 \times 10^4 (\Omega \text{ cm})^{-1}$.³¹

At concentrations larger than x_{ms} Si behaves as a semiconductor and population of the virtual bound state increases; above 60 at. % Si the occupation of the VBS has reached the line corresponding to two electrons per Si atom, as shown in the upper part of Fig. 5. Hence between 30 and 85 at. % Si we have an alloy between a metal and a semiconductor. Although the Au concentration decreases, the free-electron effective density n_f^* as well as the electrical conductivity σ_0 remains roughly constant on alloying with silicon as shown in Fig. 2 and in the lower part of Fig. 5. Above 65 at. % Si the effective density of free electrons is even higher than the linear interpolation (dashed line in Fig. 5) predicts. This feature comes out even more clearly if we calculate the optical conductivity extrapolated to $\omega=0$ according to

$$\sigma_{\text{opt}} = \tau n_f^* \frac{e^2}{m_0} . \quad (8)$$

This is shown by the dashed line in Fig. 2. We are thus forced to the conclusion that around 80 at. % Si the conductivity is much higher for optical than for dc excitations.

If we further increase the Si content of the glassy films, then we find a second transition at a concentration x_{md} in the order of 85 at. % Si. This transition may be explained from two points of view. The first is percolation theory.³² The percolation threshold is expected at about 15 at. % Au.^{6,33} Alternatively, the transition may be viewed as a change of the Au from a metallic to a dielectric state (inverse Mott transition) as it occurs, e.g., in solutions of alkali metals in ammonia.³⁴ The reason for this transition, also known as Anderson transition, is that the overlap integral of the metal electron wave functions vanishes and

hence the electrons become localized. The minimum electrical conductivity of a metal before undergoing such a transition was calculated by Mott³⁵ to about $1000 (\Omega \text{ cm})^{-1}$, which agrees quite well with our measurements (see Fig. 2). If we consider the Si as a mere background without influence on the mechanism of the transition, then we can estimate the critical density of Au atoms using the criterion given by Mott³⁵

$$U = 2z_m I . \quad (9)$$

Here U is the interatomic energy which is approximately equal to the difference between the ionization potential and the electron affinity,³⁵ or about 6.7 eV for Au. I is the overlap integral and z_m is the coordination number of the metal which is taken equal to 6 over the whole range. The metal atoms are assumed to have hydrogenlike wave functions with an atomic radius of 1.35 Å.¹⁰ For s states the overlap integral I as a function of the interatomic distance is given by Slater.³⁶ Using Eq. (9) we find that the Anderson transition occurs at an interatomic distance $d=8.0$ Å, corresponding to a concentration of 13 at. % Au embedded in an amorphous background of Si according to

$$\left(\frac{d}{d_0} \right)^3 = \frac{N_0}{N} . \quad (10)$$

Here N and N_0 are the atomic densities corresponding to the interatomic distances d and $d_0=4.1$ Å, respectively. Another criterion for the same phenomenon, given by Mott,^{35,37}

$$N_c^{1/3} a_H^* = 0.26 , \quad (11)$$

where N_c is the critical atomic density and a_H^* the empirical atomic radius.¹⁰ This for Au leads to a critical Au content of 14 at. %.¹⁰ These predictions compare favorably with Figs. 2 and 5 from which we would put the transition somewhere between 85 and 90 at. % Si. We cannot presently decide whether the percolation theory or the theory of the Anderson transition is relevant for laser-quenched Au-Si.

At Si concentrations above 85 at. % the electrical conductivity sharply decreases and the behavior is that of a heavily doped amorphous semiconductor. It may be mentioned that the conductivity of the Au-Si glasses in this region is smaller by at least 1 order of magnitude than that of Au-doped crystalline Si.

As mentioned before, some of our optical data differ from those of Hauser *et al.*⁴ At a concentration of 50 at. % Si our Au-Si glass shows a distinct reflectivity minimum (see Fig. 1) resulting in a resonance peak in the absorption at 3.4 eV [see Fig. 6(b)]. This resonance is also characteristic of amorphous Si.²⁰ No such peak is found for the 50 at. % film of Hauser *et al.*, who expect the appearance of nonmetallic behavior only for films containing more than 50–70 at. % Si.⁶ This discrepancy may indicate structural differences between the two kinds of amorphous structures, but it may also be due to residual compositional variations in the laser-quenched films.

VI. SUMMARY

Measurements of the reflectivity and the electrical conductivity of glassy Au-Si films covering the entire phase diagram were performed. The complex dielectric function calculated from Kramers-Kronig analysis is presented.

The optical data are interpreted in terms of a classical model containing essentially one bound-electron and one free-electron term. The fitted model reproduces the measured reflectivity spectra very accurately. Physically, the variation of the optical and electrical behavior is interpreted in terms of two transitions: a metal-semiconductor transition of Si and a metal-nonmetal transition of Au. These transitions occur at concentrations of about 30 and

85 at. % Si, respectively. Below 30 at. % Si the glasses behave as metallic alloys, from 30 to 85 at. % Si as alloys between a metal and a semiconductor, and above 85 at. % Si as heavily doped amorphous semiconductors.

ACKNOWLEDGMENTS

We thank N. Baltzer and K. Affolter for helpful discussions and Professor H. P. Weber for interest and support. Technical assistance of R. Flück is gratefully acknowledged. This work was supported in part by the Swiss Commission for the Encouragement of Scientific Research.

- ¹M. von Allmen, in *Glassy Metals II*, Vol. 53 of *Topics in Applied Physics*, edited by H. Beck and H.-J. Güntherodt (Springer, Heidelberg, in press).
- ²M. von Allmen, S. S. Lau, M. Mäenpää, and B. Y. Tsauro, *Appl. Phys. Lett.* **36**, 205 (1980).
- ³P. Mangin, G. Marchal, C. Mourey, and C. Janot, *Phys. Rev. B* **21**, 3047 (1980).
- ⁴E. Hauser, R. J. Zirke, and J. Tauc, *Phys. Rev. B* **19**, 6331 (1979).
- ⁵J. J. Hauser and J. Tauc, *Phys. Rev. B* **17**, 3371 (1978).
- ⁶E. Hauser, J. Tauc, and J. J. Hauser, *Solid State Commun.* **32**, 385 (1979).
- ⁷N. Nishida, M. Yamaguchi, T. Furubayashi, K. Morigaki, H. Ishimoto, and K. Ono, *Solid State Commun.* **44**, 305 (1982).
- ⁸A. Hiraki, A. Shimizu, and M. Iwami, *Appl. Phys. Lett.* **26**, 57 (1975).
- ⁹B. Stritzker and H. Wühl, *Z. Phys.* **243**, 361 (1971).
- ¹⁰K. Morigaki, *Philos. Mag. B* **42**, 979 (1980).
- ¹¹M. Born and E. Wolf, *Principles of Optics* (Pergamon, Oxford, 1975), p. 628.
- ¹²J. C. Miller, *Philos. Mag.* **20**, 1115 (1969).
- ¹³M. von Allmen and M. Mäenpää (private communication).
- ¹⁴J. J. Hauser, R. J. Schutz, and W. M. Augustyniak, *Phys. Rev. B* **18**, 3890 (1978).
- ¹⁵R. D. Swenson and U. Even, *Phys. Rev. B* **24**, 5743 (1981).
- ¹⁶A. V. Grosse, *Rev. Hautes Temp. Refract.* **3**, 115 (1966).
- ¹⁷K. P. Ackermann, M. Liard, and H.-J. Güntherodt, *J. Phys. F* **10**, L51 (1980).
- ¹⁸The concept of virtual bound states was introduced by Friedel (Ref. 38) and Anderson (Ref. 39) and was originally used to describe the behavior of bound *d* electrons of transition metals, dilutely alloyed into *s-p* metals (Ref. 40).
- ¹⁹G. E. Jellison, Jr. and F. A. Modine, *J. Appl. Phys.* **53**, 3745 (1982).
- ²⁰D. T. Pierce and W. A. Spicer, *Phys. Rev. B* **5**, 3017 (1972).
- ²¹H. Ehrenreich and H. R. Philipp, *Phys. Rev.* **128**, 1622 (1962).
- ²²*American Institute of Physics Handbook* (McGraw-Hill, New York, 1972), pp. 6–136.
- ²³H. U. Künzi and H.-J. Güntherodt, in *The Hall Effect and Its Applications* (Plenum, New York, 1980).
- ²⁴This is in contrast to the fact that Si has four valency electrons. However, amorphous Si, as mentioned above, shows only one significant resonance in the optical absorption while crystalline Si shows two.
- ²⁵In the high-frequency region (plasma region) the number of optically active electrons in crystalline Si approaches four per atom (Ref. 41). These electrons show essentially free-electron behavior. However, our measurements from 1.5–5.4 eV are far below the plasma region.
- ²⁶R. Lässer and N. V. Smith, *Phys. Rev. B* **24**, 1895 (1981).
- ²⁷D. E. Aspnes, E. Kinsbron, and D. D. Bacon, *Phys. Rev. B* **21**, 3290 (1980).
- ²⁸J. H. Mooij, *Phys. Status Solidi A* **17**, 521 (1973).
- ²⁹P. J. Cote and L. V. Meisel, in *Glassy Metals I*, Vol. 46 of *Topics in Applied Physics*, edited by H.-J. Güntherodt and H. Beck (Springer, Heidelberg, 1982).
- ³⁰K. M. Shvarev, B. A. Baum, and P. V. Gel'd, *Fiz. Tverd. Tela Leningrad* **16**, 3246 (1974) [*Sov. Phys.—Solid State* **16**, 2111 (1975)].
- ³¹O. Dreirach, R. Evans, H.-J. Güntherodt, and H. U. Künzi, *J. Phys. F* **2**, 709 (1972).
- ³²M. Pollak, in *Metal–Non-Metal Transitions in Disordered Systems*, edited by L. Friedman and D. Finlayson (Scottish University Summer Schools in Physics, Edinburgh, 1978).
- ³³R. Zallen and H. Scher, *Phys. Rev. B* **4**, 4471 (1971).
- ³⁴J. Jortner and M. H. Cohen, *Phys. Rev. B* **13**, 1548 (1976).
- ³⁵N. F. Mott, *Metal–Insulator Transitions* (Taylor and Francis, London, 1974).
- ³⁶J. C. Slater, *Quantum Theory of Matter* (McGraw-Hill, New York, 1968), Chap. 21.
- ³⁷P. P. Edwards and M. J. Sienco, *Phys. Rev. B* **17**, 2575 (1978).
- ³⁸J. Friedel, *Nuovo Cimento Suppl.* **7**, 287 (1958).
- ³⁹P. W. Anderson, *Phys. Rev.* **124**, 41 (1961).
- ⁴⁰K. P. Ackermann, Ph.D. thesis, University of Basel, Switzerland, 1979 (unpublished).
- ⁴¹H. R. Philipp and H. Ehrenreich, *Phys. Rev.* **129**, 1550 (1963).